Connecting the one-band and three-band Hubbard models of cuprates via spectroscopy and scattering experiments

K. Sheshadri [1], D. Malterre,[2] A. Fujimori [3,4,5] and A. Chainani [5]

[1]*226, Bagalur, Bangalore North, Karnataka State, 562149, India*

[2]*Institut Jean Lamour, Université de Lorraine, UMR 7198 CNRS, BP70239, 54506 Vandoeuvre lés Nancy, France*

[3]*Department of Physics, The University of Tokyo, 7-3-1 Hongo, Bunkyo-ku, Tokyo 113-0033, Japan*

[4]*Center for Quantum Science and Technology and Department of Physics, National Tsing Hua University, Hsinchu 30013, Taiwan*

[5]*Condensed Matter Physics Group, National Synchrotron Radiation Research Center, Hsinchu 30076, Taiwan*

(Received 28 October 2022; revised 8 January 2023; accepted 25 January 2023; published 15 February 2023)

The one- and three-band Hubbard models which describe the electronic structure of cuprates indicate very different values of effective electronic parameters, such as the on-site Coulomb energy and the hybridization strength. In contrast, a comparison of electronic parameters of several cuprates with corresponding values from spectroscopy and scattering experiments indicates similar values in the three-band and cluster model calculations used to simulate experimental results. The Heisenberg exchange coupling J obtained by a downfolding method in terms of the three-band parameters is used to carry out an optimization analysis consistent with J from neutron scattering experiments for a series of cuprates. In addition, the effective one-band parameters $\tilde{U}$ and $\tilde{t}$ are described using the three-band parameters, thus revealing the hidden equivalence of the one- and three-band models. The ground-state singlet weights obtained from an exact diagonalization elucidates the role of Zhang-Rice singlets in the equivalence. The results provide a consistent method to connect electronic parameters obtained from spectroscopy and the three-band model with values of J obtained from scattering experiments, band dispersion measurements, and the effective one-band Hubbard model.

DOI: 10.1103/PhysRevB.107.085125

I. INTRODUCTION

The mechanism of high-temperature superconductivity exhibited by the copper-oxide families of layered compounds remains one of the most intriguing and challenging topics in condensed matter physics [1], nearly 36 years after its discovery [2]. The discovery of copper-oxide-based superconductivity led to unprecedented theoretical and experimental efforts to understand the phenomenon. While there have been innumerable models put forth to understand the mechanism of high-temperature superconductivity, it still remains an open problem. On the other hand, nearly all the models agree that superconductivity in copper-oxide-based materials is intimately associated with quasi-two-dimensionality (2D) and strong electron-electron correlations [1]. This is based on the fact that the CuO_2 planes are the main source of the electronic states which undergo the superconducting transition. At a very broad level, the possible mechanisms discussed in the literature span over various models including the effective one-band Hubbard model [3,4], resonating valence bond theory [5], the three-band Hubbard model [6,7], the t-J model [8], spin-fluctuation-driven pairing [9], marginal Fermi liquid [10], pair density wave model [11], and electron-phonon coupling-induced pairing which goes beyond the BCS model [12].

The simplest parent compound La_2CuO_4 is a good antiferromagnetic insulator and, upon hole-doping, undergoes a transition to a dome-shaped superconducting phase with an optimal $T_c \sim 38$ K [2]. While the long-range order is lost, $La_{2-x}Sr_xCuO_4$, as well as several other copper oxide superconductors, continues to exhibit antiferromagnetic correlations in the form of resonant modes and paramagnons in the superconducting phase [13–15]. In fact, along with superconductivity, all the families of copper-oxide superconductors also show spin- and charge-ordering phenomena [16–25] which suggests a complex coexistence of electron-phonon coupling, spin fluctuations, and electron-electron correlation effects [26,27].

The basic starting point to understand cuprate properties is often considered the 2D Hubbard model involving strong electron-electron correlations with strong Cu-O hybridization leading to the Zhang-Rice singlet (ZRS) ground state (GS) [4]. It is well known and well accepted that the parent copper-oxide materials are best described as charge-transfer insulators in the Zaanen-Sawatzky-Allen scheme [28], where the copper on-site Coulomb energy $U_d \gg \Delta$, the charge-transfer energy, and the lowest energy excitations involve the strongly hybridized Cu $3d$ and O $2p$ ZRS states. Further, hole doping in the parent compound results in oxygen hole carriers retaining the ZRS character of the lowest energy excitations [29–31].

A very important issue involves how to quantify electron-electron correlations in any transition metal compound, in general, and the cuprates, in particular [32,33]. Depending on the theoretical model, the values of electron-electron correlation strength can be very different for the same material. A

comparison of the effective one-band Hubbard model [3,4] consisting of the single antibonding band made up of the Cu $d_{x^2-y^2}$ and O p_x, p_y orbitals, and the effective three-band Hubbard model [6,7] which describes the cuprate electronic structure in terms of the Cu-O bonding, nonbonding, and antibonding bands show significantly different values of on-site Coulomb energy in the Cu d states. In the following, to distinguish the one- and three-band parameters, we use the notation U_d/U_p and t_{pd} for the Cu/O on-site Coulomb energies and hopping in the three-band model, while $\tilde{U}$ and $\tilde{t}$ are used for the one-band Hubbard model, respectively. Thus, for example, while early studies of the three-band model estimated $U_d \sim 7$–10 eV and $U_p \sim 3$–6 eV [34–36], typical values of $\tilde{U} \sim 3$–4 eV are known for the effective one-band model [37,38].

It is noted that, while several theoretical studies have included the oxygen on-site Coulomb energy U_p, there are also some studies which have neglected U_p. For example, early theory [7] and cluster model calculations of core-level photoemission and optical absorption [39–42] could explain experimental results fairly well but in the absence of U_p. In a study using the coherent potential approximation, an effective one-band model was obtained from the three-band model including the intersite Coulomb energy U_{pd} treated in the Hartree-Fock approximation, but with $U_p = 0$ [43,44]. The authors showed that the effective $\tilde{U}$ increased on increasing U_{pd}, and they could obtain a metal-insulator phase diagram as a function of U_d and Δ. In a three-band Hubbard model using the constrained-path Monte Carlo method, the binding energy of a pair of holes and the symmetry of superconducting pairing correlation functions was investigated but in the absence of U_p [45]. Cluster perturbation theory applied to calculate spectral functions of cuprates also did not include U_p but could show spin-charge separation in the one-dimensional (1D) Hubbard model, as well as momentum-dependent spectral-weight in the 2D Hubbard model [46]. Cluster dynamical mean field theory approximation was used to investigate the three-band Hubbard model in the absence of U_p and showed that the cuprates can be described as magnetically correlated Mott insulators [47]. More recently, quantum Monte Carlo calculations demonstrated dynamical stripe correlations in the three-band Hubbard model without U_p and explained experimental observations such as the hourglass magnetic dispersion [48]. The three-band Hubbard model using the auxiliary-field quantum Monte Carlo method, but without U_p, was used to show the importance of Δ and a quantum phase transition from an antiferromagnetic insulator to paramagnetic metal for $\Delta < 3$ eV [49].

However, electron spectroscopy studies in conjunction with cluster model calculations or using the Cini-Sawatzky method [50,51] have estimated $U_d \sim 6$–8 eV [39,40,52] and $U_p \sim 5$–6 eV [53–55]. Thus, U_d and U_p are comparable and needed for describing the electronic states derived from Cu-O planes, particularly in the charge transfer limit, as U_p gets close to or larger than Δ. Further, an *ab initio* method with dynamical screening [37] applied to the one-band model for La_2CuO_4 estimated a static $\tilde{U}(w = 0) \sim 3.65$ eV, while for the three-band model, it gave $U_d(w = 0) \sim 7.0$ eV and $U_p(w = 0) \sim 4.64$ eV. Another very recent multiscale *ab initio* method [38] applied to the one-band model for La_2CuO_4 estimated $\tilde{U} \sim 5.0$ eV, while for the three-band model, it estimated $U_d \sim 9.6$ eV and $U_p \sim 6.1$ eV. It is noted that the models have also estimated the intersite Coulomb energies, as well as the nearest-neighbor (NN) and next-NN hopping (t and t') which also show differences depending on the method [34–38].

Very interestingly, Hubbard-type cluster models employing $d_{x^2-y^2}$, p_x, and p_y levels have been extensively used for calculating spectra in high-energy spectroscopies like core-level photoemission (PES) and x-ray absorption, and resonant inelastic x-ray scattering (RIXS) structure factors, and the obtained electronic parameters [53–71] are quite close to the theoretical estimates from the effective three-band model [34–36,38,72] (see Tables I and II). It is noted that the effective three-band model parameters were also used to calculate the dynamical spin structure factor of Bi2201 measured by RIXS [65]. On the other hand, analysis of neutron scattering measurements of magnon dispersions [73] and angle-resolved PES (ARPES) band dispersions [74,75] of parent cuprates have employed the extended one-band Hubbard model or the extended $t - J$ model to study the NN exchange interaction and correlation effects, and they obtained electronic parameter values close to the values obtained from the effective one-band theoretical models.

For example, it was shown that neutron scattering of La_2CuO_4 provided a dominant NN hopping $t = 0.33$ eV and an effective $U/t = 8.8$ with $U = 2.9$ eV but also showed that, in addition to the NN exchange $J = 138$ meV, it was important to include ring exchange $J_c = 38$ meV, while $J' = J'' = 2$ meV were small [73]. Similarly, for $Sr_2CuO_2Cl_2$, the $t - t' - t'' - J$ model showed $t = 0.35$ eV, while $t' = 0.12$ eV, and $t'' = 0.08$ eV, and with a $J = 0.14$ eV [75], it implied an effective $\tilde{U}/t = 10$ with $\tilde{U} = 3.5$ eV. Thus, in these cases, the results suggest that the NN hopping t and U can be considered the $\tilde{t}$ and $\tilde{U}$ of the one-band model. For CuO, a recent study showed that a linear spin-wave model for a Heisenberg antiferromagnet provided a good description of the neutron scattering results [76]. The relevant exchange constants could be accurately determined and showed that the dominant exchange interaction $J = 91$ meV, which coupled antiferromagnetically along the $[10\bar{1}]$ chain direction, while the NN interchain interactions were very weak ($J_{ac} = 3.9$ meV and $J_b = 0.39$ meV) and coupled ferromagnetically [76].

Given the differences in electronic parameters between the theoretical one-band vs the three-band models and the corresponding experimental high-energy spectroscopies vs the low-energy magnon and band dispersion measurements, we felt it important to address a possible connection between them. In this paper, we have found an equivalence by using the NN Heisenberg exchange interaction J obtained from neutron scattering and RIXS experiments [59–65,73,76] as a bridge to connect electronic parameters known from experiment (high-energy spectroscopy, RIXS, and neutron scattering) and theoretical estimates obtained from the one- and three-band Hubbard models. The results show that the three-band Hubbard model parameters can be used to describe J in terms of the well-known one-band Hubbard model form of $J = 4\tilde{t}^2/\tilde{U}$ with renormalized parameters $\tilde{U}$ and $\tilde{t}$.

We now summarize our main results. We calculate J, the strength of the Heisenberg coupling between Cu moments in

TABLE I. Electronic parameters (U_d, t_{pd}, Δ, and U_p) for cuprates from the three-band Hubbard model (theory) and from cluster model calculations (spectroscopy and RIXS). The table also shows two optimized parameter sets (Δ_1, U_{p1} and t_{pd2}, Δ_2) with their cost functions f_1 and f_2, respectively. J is the NN Heisenberg exchange deduced from scattering experiments. See text for details.

					Optimization-1				Optimization-2		
Compound [Ref.]	U_d (±0.5 eV)	t_{pd} (±0.2 eV)	Δ (±1.0 eV)	U_p (±0.5 eV)	Δ_1 (eV)	U_{p1} (eV)	f_1	J [Ref.] (±5 meV)	t_{pd2} (eV)	Δ_2 (eV)	f_2
Theory											
La_2CuO_4 [34]	9.4	1.5	3.5	4.7	5.7	4.9	5.09	140 [73]	1.1	3.7	0.96
La_2CuO_4 [35]	10.5	1.3	3.6	4.0	4.5	4.1	1.01	140 [73]	1.2	3.7	0.4
La_2CuO_4 [36]	8.8	1.3	3.5	6.0	4.5	6.1	0.98	140 [73]	1.2	3.7	0.38
La_2CuO_4 [38]	9.61	1.37	3.7	6.1	4.6	6.2	0.79	140 [73]	1.2	3.9	0.36
Hg1201 [38]	8.84	1.26	2.42	5.3	4.4	5.4	3.78	135 [64]	0.9	2.6	0.75
Bi2212 [72]	8.5	1.13	3.2	4.1	3.5	4.1	0.06	161 [64]	1.1	3.5	0.06
Spectroscopy											
CuO [54,69]	7.7	1.55	2.5	5	7.6	5.4	25.9	91 [76][a]	0.8	2.6	1.72
Sr_2CuO_3 [66,67]	8.8	1.45	2.5	4.4	4.4	4.6	3.62	241 [59]	1.1	2.8	0.96
$Sr_2CuO_2Cl_2$ [68]	8.8	1.5	3.5	4.4	6.0	4.6	6.45	130 [74,75]	1.1	3.7	1.04
La_2CuO_4 [69,70]	7.0	1.5	3.5	6.0	6.0	6.2	6.49	140 [73]	1.13	3.7	1.0
Nd_2CuO_4 [71]	8.0	1.1	3.0	4.1	3.6	4.1	0.41	133 [60]	1.0	3.2	0.21
Pr_2CuO_4 [71]	8.0	1.1	3.0	4.1	3.8	4.2	0.62	121 [60]	1.0	3.2	0.26
YBCO [53,55]	7.0	1.2	1.5	5.0	4.4	5.2	8.2	125 [61]	0.7	1.7	0.99
Bi2212 [58]	7.7	1.5	3.5	6.0	5.6	6.1	4.3	161 [64]	1.2	3.7	0.88
RIXS											
Bi2201 [65]	10.2	1.35	3.9	5.9	4.5	5.9	0.34	153 [64,65]	1.3	4.1	0.22

[a]For CuO, the dominant exchange interaction J which couples antiferromagnetically is the one along the $[10\bar{1}]$ chain direction and considered here, while the NN spins exhibit a weak ferromagnetic coupling.

a Cu_2O cluster, using the downfolding method discussed by Koch [33]. For several compounds, neutron scattering data for J and spectroscopic data for U_d, U_p, Δ, and t_{pd} are available. Directly using the spectroscopic parameter values in the downfolding expression for J leads to deviations from the experimental J values. We therefore use two estimation

TABLE II. Renormalized electronic parameters $\tilde{U}$ and $\tilde{t}$ for cuprates in the one-band Hubbard model along with the GS singlet weights c_{21} (between the two Cu sites) and c_{13} (between the Cu and O site). Optimization-1 uses U_d, t_{pd}, Δ_1, and U_{p1}; and Optimization-2 uses U_d, t_{pd2}, Δ_2, and U_p from Table I to obtain corresponding $\tilde{U}$ and $\tilde{t}$.

	Optimization-1				Optimization-2				
Compound [Ref.]	$\tilde{U}$ (eV)	$\tilde{t}$ (eV)	$\tilde{U}/\tilde{t}$	J (meV)	$\tilde{U}$ (eV)	$\tilde{t}$ (eV)	$\tilde{U}/\tilde{t}$	c_{21}	c_{13}
Theory									
La_2CuO_4 [34]	4.38	0.39	11.18	140	3.68	0.36	10.26	0.65	0.2
La_2CuO_4 [35]	4.03	0.37	10.73	140	3.7	0.36	10.28	0.65	0.2
La_2CuO_4 [36]	4.05	0.38	10.76	140	3.81	0.37	10.42	0.64	0.2
La_2CuO_4 [38]	4.27	0.41	10.43	140	4.05	0.4	10.16	0.64	0.2
Hg1201 [38]	3.93	0.36	10.79	135	3.3	0.33	9.89	0.63	0.21
Bi2212 [72]	3.35	0.37	9.13	161	3.34	0.37	9.11	0.64	0.2
Spectroscopy									
CuO [54,69]	4.39	0.32	13.87	91	3.09	0.27	11.62	0.64	0.2
Sr_2CuO_3 [66,67]	3.79	0.48	7.94	241	3.17	0.44	7.25	0.62	0.23
$Sr_2CuO_2Cl_2$ [68]	4.28	0.37	11.47	130	3.53	0.34	10.42	0.65	0.19
La_2CuO_4 [69,70]	3.96	0.37	10.64	140	3.42	0.34	9.89	0.64	0.2
Nd_2CuO_4 [71]	3.33	0.33	10.01	133	3.17	0.32	9.75	0.64	0.2
Pr_2CuO_4 [71]	3.38	0.32	10.58	121	3.16	0.31	10.23	0.64	0.2
YBCO [53,55]	3.49	0.33	10.56	125	2.61	0.29	9.14	0.62	0.23
Bi2212 [58]	4.07	0.4	10.05	161	3.59	0.38	9.44	0.64	0.2
RIXS									
Bi2201 [65]	4.31	0.41	10.61	153	4.18	0.4	10.45	0.65	0.2

procedures, referred to as Optimization-1 and Optimization-2 in the following, to modify a subset (different in the two procedures) of the spectroscopic data, so that there is good agreement with experimental J values using the procedure described in Sec. II. We identify effective parameters $\tilde{t}$ and $\tilde{U}$ so that the downfolding expression for J becomes equal to $4\tilde{t}^2/\tilde{U}$. The estimated values of $\tilde{t}$ and $\tilde{U}$ are found to be consistently smaller than t_{pd} and U_d in all cases but lead to a larger $\tilde{U}/\tilde{t}$ in the one-band case compared with U_d/t_{pd} of the three-band case, in good agreement with theoretical estimates reported in the literature. The results indicate that stronger effective correlations, arising from a combination of U_d, U_p, Δ, and t_{pd} are hidden in the effective one-band Hubbard model. In this paper, we provide a consistent method to connect electronic parameters obtained from spectroscopy and the three-band model with effective parameters obtained from neutron scattering, ARPES measurements, and the one-band Hubbard model.

II. CALCULATIONS

We consider a Cu_2O cluster with site labels $i = 1, 2$ [for Cu(1) and Cu(2) atoms] and $i = 3$ (for the O atom). The cluster Hamiltonian is

$$\hat{H} = \frac{\Delta}{2}(n_3 - n_1 - n_2) - t_{pd}\sum_{i\sigma}(d^\dagger_{i\sigma}p_\sigma + \text{H.c.}) + U_d(n_{1\uparrow}n_{1\downarrow} + n_{2\uparrow}n_{2\downarrow}) + U_p n_{3\uparrow}n_{3\downarrow}, \tag{1}$$

where $n^d_{i\sigma} = d^\dagger_{i\sigma}d_{i\sigma}$ $(i = 1, 2)$, $n_{3\sigma} = p^\dagger_\sigma p_\sigma$, and $n_i = n_{i\uparrow} + n_{i\downarrow}$. Here, $d^\dagger_{i\sigma}$ creates a hole with a z component of spin $\sigma = \pm\frac{1}{2}$ in the Cu d orbital at site i $(= 1, 2)$, and $p^\dagger_\sigma$ creates a hole with a z component of spin $\sigma = \pm\frac{1}{2}$ in the O p orbital at the site located in between the two Cu sites. Here, Δ is the charge-transfer energy; the parameters U_p and U_d are on-site Coulomb energies at the O and Cu sites, respectively; and finally, t_{pd} is the strength of hopping between neighboring O and Cu sites.

In this paper, we consider a filling fraction corresponding to undoped cuprates, in which the outermost p orbital on the O site is filled with two electrons (i.e., empty in the hole picture), and the outermost d orbital on the Cu site has one electron (i.e., one hole), in the absence of hopping. For our cluster with three atoms, this corresponds to a total occupancy of four electrons or two holes. The two holes can be selected in three ways: both with $\sigma = -\frac{1}{2}$ (the ferromagnetic down case), both with $\sigma = \frac{1}{2}$ (the ferromagnetic up case), and finally, one hole with $\sigma = \frac{1}{2}$ and another with $\sigma = -\frac{1}{2}$ (the antiferromagnetic case).

We will consider only the antiferromagnetic case henceforth. In this case, there are nine basis states $|i, j\rangle$, $i, j = 1, 2, 3$. In state $|i, j\rangle$, i and j are the Cu $(i, j = 1, 2)$ or O $(i, j = 3)$ sites with up and down holes, respectively. In the basis $\{|1, 2\rangle, |2, 1\rangle, |1, 3\rangle, |3, 1\rangle, |2, 3\rangle, |3, 2\rangle, |1, 1\rangle, |2, 2\rangle, |3, 3\rangle\}$, the Hamiltonian in Eq. (1) becomes a 9×9 matrix:

$$H = \begin{bmatrix} H_{00} & H_{01} & H_{02} \\ H_{10} & H_{11} & H_{12} \\ H_{20} & H_{21} & H_{22} \end{bmatrix}, \tag{2}$$

in which the blocks are

$$H_{00} = -\Delta\begin{bmatrix} 1 & 0 \\ 0 & 1 \end{bmatrix}, \quad H_{01} = \begin{bmatrix} t_{pd} & 0 & 0 & -t_{pd} \\ 0 & t_{pd} & -t_{pd} & 0 \end{bmatrix},$$
$$H_{02} = O_{2\times 3}, \quad H_{11} = O_{4\times 4},$$
$$H_{12} = \begin{bmatrix} t_{pd} & 0 & t_{pd} \\ -t_{pd} & 0 & -t_{pd} \\ 0 & t_{pd} & t_{pd} \\ 0 & -t_{pd} & -t_{pd} \end{bmatrix},$$
$$H_{22} = \begin{bmatrix} U_d - \Delta & 0 & 0 \\ 0 & U_d - \Delta & 0 \\ 0 & 0 & U_p + \Delta \end{bmatrix}. \tag{3}$$

In the above, $O_{m\times n}$ denotes an $m \times n$ matrix of zeros. We calculate the Heisenberg antiferromagnetic coupling J between the Cu(1) and Cu(2) spins based on the downfolding fourth-order perturbation method described by Koch [33] and Zurek [77]. Accordingly, the effective Hamiltonian is

$$\begin{aligned}\tilde{H} &= H_{00} + H_{01}\{\epsilon - [H_{11} + H_{12}(\epsilon - H_{22})^{-1}H_{21}]^{-1}\}^{-1}. \\ &\approx H_{00} + H_{01}(\epsilon - H_{11})^{-1}H_{10} + H_{01}(\epsilon - H_{11})^{-1} \\ &\quad \times H_{12}(\epsilon - H_{22})^{-1}H_{21}(\epsilon - H_{11})^{-1}H_{10},\end{aligned} \tag{4}$$

where we have used the approximation $(A + B)^{-1} \approx A^{-1}(1 - BA^{-1})$. We now take $\epsilon = -\Delta$ and perform the matrix products above. The result is

$$\tilde{H} \approx -\frac{2t^2_{pd}}{\Delta}\begin{bmatrix} 1 & 0 \\ 0 & 1 \end{bmatrix} - \frac{J}{2}\begin{bmatrix} 1 & -1 \\ -1 & 1 \end{bmatrix}, \tag{5}$$

where the Heisenberg coupling is

$$J = 4\frac{t^4_{pd}}{\Delta^2}\left[\frac{1}{U_d} + \frac{1}{\Delta + U_p/2}\right]. \tag{6}$$

The result we have obtained for J using the downfolding approximation is the same as that reported in earlier studies [32,78,79] using a fourth-order perturbation theory. If we now define $\tilde{t}$ and $\tilde{U}$ using

$$\tilde{t} = \frac{t^2_{pd}}{\Delta}, \quad \frac{1}{\tilde{U}} = \frac{1}{U_d} + \frac{1}{\Delta + U_p/2}, \tag{7}$$

then $J = 4\tilde{t}^2/\tilde{U}$. This is the expression for J we would get if we used a one-band Hubbard model with a hopping strength $\tilde{t}$ and an on-site repulsion $\tilde{U} \gg \tilde{t}$, using second-order perturbation theory. In this sense, we consider $\tilde{U}$ and $\tilde{t}$ as the parameters of an effective one-band Hubbard model corresponding to the model in Eq. (1).

We find that using the spectroscopic values on the right-hand side and the experimental J values on the left-hand side of Eq. (6) does not satisfy the equation with sufficient accuracy. We therefore modify, in an optimal manner described below, a subset of the spectroscopic parameter values so that the agreement is good.

We now describe two such simple optimization procedures. We define the parameter $R = \tilde{U}/\tilde{t}$ to obtain the parametric forms $\tilde{t} = RJ/4$, $\tilde{U} = R^2J/4$ for the effective parameters. These are the expressions that we use below for $\tilde{t}$, $\tilde{U}$.

TABLE III. Examples of one-band model electronic parameters estimated independently from magnon dispersion in neutron scattering, band dispersion in ARPES, and from *ab initio* theory.

Compound [Ref.]	$\tilde{U}$ (eV)	$\tilde{t}$ (eV)	$\tilde{U}/\tilde{t}$	Method
La_2CuO_4 [79]	2.9	0.33	8.8	Neutron scattering
$Sr_2CuO_2Cl_2$ [73,80]	3.5	0.35	10.0	ARPES
La_2CuO_4 [38]	5.0	0.48	10.4	*Ab initio* theory
Hg1201 [38]	4.4	0.46	9.5	*Ab initio* theory

In the Optimization-1 procedure, we modify $(\Delta,\ U_p)$. We solve the relations in Eq. (7) to obtain $\Delta_1(R) = t_{pd}^2/\tilde{t}$ and $U_{p1}(R)/2 = U_d\tilde{U}/(U_d - \tilde{U}) - \Delta_1(R)$. We then minimize a cost function $f_1(R) = [\Delta_1(R) - \Delta]^2 + [U_{p1}(R) - U_p]^2$ with respect to R to obtain the minimum $R^\star$, using the spectroscopic values for U_d, U_p, Δ, and t_{pd} and neutron scattering values for J. This estimates $\Delta_1(R^\star)$, $U_{p1}(R^\star)$, $\tilde{U}(R^\star)$, and $\tilde{t}(R^\star)$.

In the Optimization-2 procedure, we modify $(\Delta,\ t_{pd})$. We solve the relations in Eq. (7) to obtain $t_{pd2}(R)^2 = \Delta_2(R)\tilde{t}$ and $\Delta_2(R) = U_d\tilde{U}/(U_d - \tilde{U}) - U_p/2$. We then minimize a cost function $f_2(R) = [\Delta_2(R) - \Delta]^2 + |[t_{pd2}(R)^2 - t_{pd}^2]|$ with respect to R to obtain the minimum $R^\star$, using the spectroscopic values for U_d, U_p, Δ, and t_{pd} and neutron scattering values for J. This estimates $\Delta_2(R^\star)$, $t_{pd2}(R^\star)$, $\tilde{U}(R^\star)$, and $\tilde{t}(R^\star)$.

III. RESULTS AND DISCUSSION

The results are summarized in Tables I and II for a variety of CuO-based materials. Table I presents our estimates of the theoretical and spectroscopic three-band model parameters, while Table II presents our estimates of effective one-band parameters. Both tables contain results of the two optimization procedures that we discussed above.

In Table I, columns 5–7 present results of the Optimization-1 procedure: These are values of Δ_1, U_{p1}, and f_1. Columns 9–11 present results of the Optimization-2 procedure: These are values of t_{pd2}, Δ_2, and f_2. We can see from the cost function values that Optimization-2 is better than Optimization-1; this is also reflected in the greater closeness of (t_{pd2}, Δ_2) estimates to measured values than that of (Δ_1, U_{p1}) estimates to measured values. Considering that J depends on t_{pd}^4 in Eq. (6), it can be seen that a smaller spread in t_{pd} across compounds provides a better description of parameter values; further, since Δ and t_{pd} are intimately related through the first relation in Eq. (7), it makes sense to optimize with respect to these two parameters as is done in Optimization-2. This has the result of reducing the spread in estimated t_{pd2} values compared with reported spectroscopic t_{pd} values. This also improves the estimates of Δ compared with Δ_1 in Optimization-1. For these reasons, we can understand that Optimization-2 is better than not only Optimization-1 but also other possible optimization choices, namely, (Δ, U_d), (t_{pd}, U_p), and (t_{pd}, U_d). We therefore do not present the results of these latter procedures.

Since $R = \tilde{U}/\tilde{t} \sim 10$ in most cases (see columns 4 and 8 in Table II), we can see that it makes sense to treat $\tilde{U}$, $\tilde{t}$ as effective one-band parameters, as is known from earlier work (Table III). We observe that $R \sim 10$ not only in cases where spectroscopic three-band parameter values are reported but also for theoretical as well as RIXS three-band parameter values (see Table II).

Secondly, $\tilde{U}$ is roughly half of U_d in almost all cases. This shows that the effective model is not a simple Cu d-band model, but possibly a more hybrid one involving Cu d and O (p_x, p_y) orbitals. To understand this better, we have looked at the nature of the GS obtained by exactly diagonalizing the cluster Hamiltonian in Eq. (1) for each compound in Table I using our Optimization-2 estimates of the three-band parameters. The GS we obtain, $|G\rangle = \sum_{ij} c_{ij}|i, j\rangle$, always has the property $c_{12} = -c_{21}, c_{13} = -c_{31} = c_{23} = -c_{32}, c_{11} = c_{22}$ by symmetry, which shows that it is a singlet of Cu and O orbitals. We can thus completely characterize the GS with the two distinct singlet weights c_{21} and c_{13} and the two distinct hole double-occupancy weights c_{11} and c_{33}. Since our focus is primarily on the singlet nature of $|G\rangle$, we present c_{21} and c_{13} in Table II (see columns 9 and 10). The singlet weights of the Cu-Cu and Cu-O sectors confirm that the GS is a ZRS. The effective interaction $\tilde{U}$ is thus not between purely Cu d holes but represents the hybrid ZR singlets and is therefore significantly smaller than U_d. However, it must also be noted from Tables I and II that $\tilde{U}/\tilde{t} \simeq 10$, satisfying the strong correlation condition in the effective one-band model. In Table III, we list a few examples of one-band model electronic parameters estimated independently, from magnon dispersion in neutron scattering, band dispersion in ARPES, and from *ab initio* theory. It is clear that the values of $\tilde{U}/\tilde{t}$ in all the cases are close to the values in Table II and validate our analysis.

Finally, in Figs. 1(a)–1(d), we present plots of various $|c_{ij}|^2$ as a function of t_{pd}, for $U_p = 1$, 3, and 5 eV; we have fixed the values $U_d = 8$ eV and $\Delta = 3.3$ eV (=average Δ of values obtained by Optimization-2 shown in Table I) in these plots. Figure 1(a) shows that the pure Cu(1)-Cu(2) singlet weight $2|c_{12}|^2 \sim 1$ obtained for $t_{pd} = 0$ systematically reduces in weight on increasing t_{pd}. Simultaneously, the total Cu(1)-O(3) singlet weight $4|c_{13}|^2$ increases systematically on increasing t_{pd}, indicating the role of Cu-O hybridization in forming the ZRS state for the cuprates. Thus, the O p orbital plays an increasingly important role on increasing t_{pd} to $\sim$1 eV, typical of the cuprates. Further, the on-site double occupancy weights $|c_{ii}|^2$, $i = 1 - 3$, are quite small [Figs. 1(c) and 1(d)]. However, on increasing U_p from 1 to 5 eV, while there is hardly any change in the total double occupancy weight $2|c_{11}|^2$ on the Cu sites, the double occupancy weight $|c_{33}|^2$ on the O site gets suppressed to nearly half its value for $t_{pd} > 1$ eV. This behavior of the O site double occupancy is closely related to the reduction of J by U_p according to Eq. (6). Thus, U_p plays an important role in tuning the value of J, which is considered one of the most important parameters to achieve high-temperature superconductivity exhibited by the family of cuprates [1,59–65,73,81–84].

IV. CONCLUDING REMARKS

In this paper, we have presented a data analysis of spectroscopic parameters and neutron scattering parameters for a variety of cuprates based on a theoretical relationship between the parameters of a three-band model and effective one-band Heisenberg antiferromagnetic coupling, using a cluster model

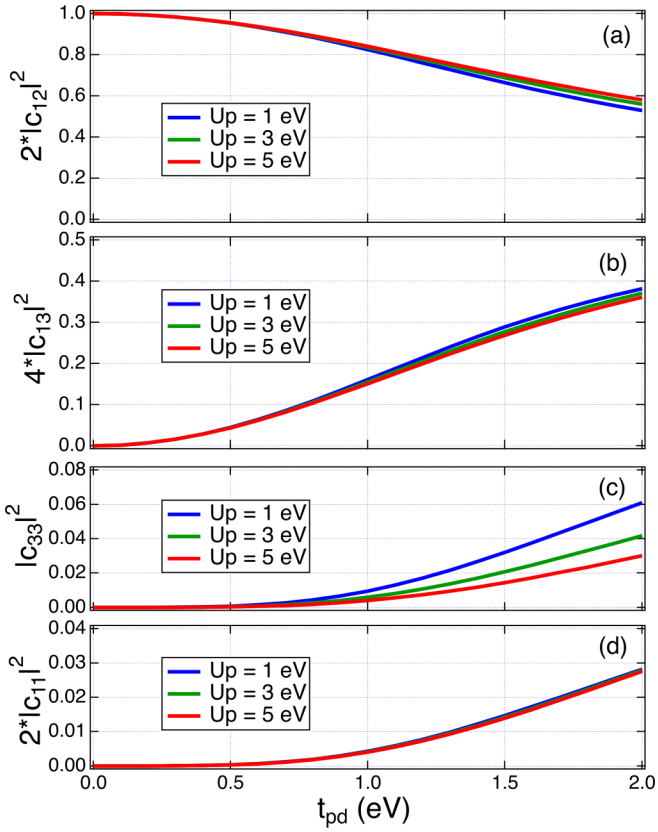

FIG. 1. Plots of various calculated total weights $|c_{ij}|^2$ as a function of t_{pd}, for $U_d = 8$ eV, $\Delta = 3.3$ eV, and $U_p = 1$, 3, and 5 eV. (a) Total Cu(1)-Cu(2) singlet weight $2|c_{12}|^2$. (b) Total Cu(1)-O(3) singlet weight $4|c_{13}|^2$. (c) and (d) On-site double occupancy weights $|2c_{11}|^2$ [total for the Cu(1) and Cu(2) sites] and $|c_{33}|^2$ for the O(3) site.

calculation. We have also performed an exact diagonalization of the cluster Hamiltonian to understand the nature of the GS.

Our analysis shows $\tilde{U} < U_d$ always. In addition to agreeing with estimates of $\tilde{U}$ from the one-band model applied to neutron scattering or ARPES experiments, this inequality is a direct consequence of Eq. (7).

Here, U_p is significant in magnitude, both in measurements and in our estimates, and is not small compared with U_d. While U_p has been neglected in some studies on cuprates, we believe it is as important as U_d. Further, the second relation in Eq. (7) shows that the effective interaction $\tilde{U}$ is enhanced by U_p and Δ.

The GS singlet weights from our exact diagonalization show the importance of O moments and ZRS in the effective description. We also observe that the singlet weights change very little across the family of compounds, despite a variation in the three-band spectroscopic parameters that are used to calculate them. This holds for the ratio $\tilde{U}/\tilde{t}$ as well.

Here, $\tilde{U}/\tilde{t} \sim 10$ in all cases, pointing to the effective one-band model being strongly correlated.

As to the spectroscopic values of the three-band parameters, it is generally believed that Δ and t_{pd} measurements are less reliable than those of U_d and U_p. Our estimation procedure Optimization-2 attempts to offer a reasonable description of the spectroscopic and neutron scattering data by reducing the spread in the values of Δ and t_{pd} across the family of cuprates.

In conclusion, we have performed a perturbative and exact diagonalization study of a model of a Cu_2O cluster that connects electronic parameters obtained from spectroscopy and the three-band model with values of J obtained from scattering, band dispersion measurements, and the effective one-band Hubbard model.

ACKNOWLEDGMENTS

A.F. thanks JSPS KAKENHI (Grants No. JP19K03741 and No. JP22K03535) and the "Program for Promoting Researches on the Supercomputer Fugaku" (Basic Science for Emergence and Functionality in Quantum Matter, No. JPMXP1020200104) from MEXT. A.C. thanks the National Science and Technology Council of the Republic of China, Taiwan, for financially supporting this research under Contract No. NSTC 111-2112-M-213-031.

[1] B. Keimer, S. A. Kivelson, M. R. Norman, S. Uchida, and J. Zaanen, From quantum matter to high-temperature superconductivity in copper oxides, Nature (London) **518**, 179 (2015).

[2] J. G. Bednorz and K. A. Mueller, Possible high T_c superconductivity in the Ba-La-Cu-O system, Z. Phys. B **64**, 189 (1986).

[3] P. W. Anderson, 50 years of the Mott phenomenon: Insulators, magnets, solids and superconductors as aspects of strong-repulsion theory, in *Frontiers and Borderlines in Many-Particle Physics, Proceedings of the International School of Physics – Enrico Fermi Course CIV*, edited by R. A. Broglia and J. R. Schrieffer (North-Holland, Amsterdam, 1988), pp. 1–40.

[4] F. C. Zhang and T. M. Rice, Effective Hamiltonian for the superconducting Cu oxides, Phys. Rev. B **37**, 3759 (1988).

[5] G. Baskaran, Z. Zou, and P. W. Anderson, The resonating valence bond state and high-T_c superconductivity—A mean field theory, Solid State Commun. **63**, 973 (1987).

[6] C. M. Varma, S. Schmitt-Rink, and E. Abrahams, Charge transfer excitations and superconductivity in "ionic" metals, Solid State Commun. **62**, 681 (1987).

[7] V. J. Emery, Theory of High-T_c Superconductivity in Oxides, Phys. Rev. Lett. **58**, 2794 (1987).

[8] J. Spałek, Effect of pair hopping and magnitude of intra-atomic interaction on exchange-mediated superconductivity, Phys. Rev. B **37**, 533 (1988).

[9] H. J. Schulz, Superconductivity and antiferromagnetism in the two-dimensional Hubbard model: Scaling theory, Europhys. Lett. **4**, 609 (1987).

[10] C. M. Varma, P. B. Littlewood, S. Schmitt-Rink, E. Abrahams, and A. E. Ruckenstein, Phenomenology of the Normal State of

Cu-O High-Temperature Superconductors, Phys. Rev. Lett. **63**, 1996 (1989).

[11] D. F. Agterberg, J. C. Seamus Davis, S. D. Edkins, E. Fradkin, D. J. Van Harlingen, S. A. Kivelson, P. A. Lee, L. Radzihovsky, J. M. Tranquada, and Y. Wang, The physics of pair density waves, Annu. Rev. Condens. Matter Phys. **11**, 231 (2020).

[12] A. R. Bishop, R. M. Martin, K. A. Muller, and Z. Tesanovic, Superconductivity in oxides: Toward a unified picture, Z. Phys. B **76**, 17 (1989).

[13] J. Rossat-Mignod, L. P. Regnault, C. Vettier, P. Bourges, P. Burlet, J. Bossy, J. Y. Henry, and G. Lapertot, Neutron scattering study of the $YBa_2Cu_3O_{6+x}$ system, Physica C **185-189**, 86 (1991).

[14] M. Eschrig, The effect of collective spin-1 excitations on electronic spectra in high-T_c superconductors, Adv. Phys. **55**, 47 (2006).

[15] M. Le Tacon, G. Ghiringhelli, J. Chaloupka, M. Moretti Sala, V. Hinkov, M. W. Haverkort, M. Minola, M. Bakr, K. J. Zhou, S. Blanco-Canosa *et al.*, Intense paramagnon excitations in a large family of high-temperature superconductors, Nat. Phys. **7**, 725 (2011).

[16] J. M. Tranquada, B. J. Sternlieb, J. D. Axe, Y. Nakamura, and S. Uchida, Evidence for stripe correlations of spins and holes in copper oxide superconductors, Nature (London) **375**, 561 (1995).

[17] T. Wu, H. Mayaffre, S. Kramer, M. Horvatic, C. Berthier, W. N. Hardy, R. Liang, D. A. Bonn, and M.-H. Julien, Magnetic-field-induced charge-stripe order in the high-temperature superconductor $YBa_2Cu_3O_y$, Nature (London) **477**, 191 (2011).

[18] G. Ghiringhelli, M. Le Tacon, M. Minola, S. Blanco-Canosa, C. Mazzoli, N. B. Brookes, G. M. De Luca, A. Frano, D. G. Hawthorn, F. He *et al.*, Long-range incommensurate charge fluctuations in (Y, Nd)$Ba_2Cu_3O_{6+x}$, Science **337**, 821 (2012).

[19] J. Chang, E. Blackburn, A. T. Holmes, N. B. Christensen, J. Larsen, J. Mesot, R. Liang, D. A. Bonn, W. N. Hardy, A. Watenphul *et al.*, Direct observation of competition between superconductivity and charge density wave order in $YBa_2Cu_3O_{6.67}$, Nat. Phys. **8**, 871 (2012).

[20] M. Le Tacon, A. Bosak, S. M. Souliou, G. Dellea, T. Loew, R. Heid, K.-P. Bohnen, G. Ghiringhelli, M. Krisch, and B. Keimer, Inelastic x-ray scattering in $YBa_2Cu_3O_{6.6}$ reveals giant phonon anomalies and elastic central peak due to charge-density-wave formation, Nat. Phys. **10**, 52 (2014).

[21] W. Tabis, Y. Li, M. Le Tacon, L. Braicovich, A. Kreyssig, M. Minola, G. Dellea, E. Weschke, M. J. Veit, M. Ramazanoglu *et al.*, Charge order and its connection with Fermi-liquid charge transport in a pristine high-T_c cuprate, Nat. Commun. **5**, 5875 (2014).

[22] S. Gerber, H. Jang, H. Nojiri, S. Matsuzawa, H. Yasumura, D. A. Bonn, R. Liang, W. N. Hardy, Z. Islam, A. Mehta *et al.*, Three-dimensional charge density wave order in $YBa_2Cu_3O_{6.67}$ at high magnetic fields, Science **350**, 949 (2015).

[23] M.-H. Julien, P. Carretta, M. Horvatic, C. Berthier, Y. Berthier, P. Segransan, A. Carrington, and D. Colson, Spin Gap in $HgBa_2Ca_2Cu_3O_{8+\delta}$ Single Crystals from ^{63}Cu NMR, Phys. Rev. Lett. **76**, 4238 (1996).

[24] W. S. Lee, J. J. Lee, E. A. Nowadnick, S. Gerber, W. Tabis, S. W. Huang, V. N. Strocov, E. M. Motoyama, G. Yu, B. Moritz *et al.*, Asymmetry of collective excitations in electron- and hole-doped cuprate superconductors, Nat. Phys. **10**, 883 (2014).

[25] M. K. Chan, C. J. Dorow, L. Mangin-Thro, Y. Tang, Y. Ge, M. J. Veit, G. Yu, X. Zhao, A. D. Christianson, J. T. Park *et al.*, Commensurate antiferromagnetic excitations as a signature of the pseudogap in the tetragonal high-T_c cuprate $HgBa_2CuO_{4+\delta}$, Nat. Commun. **7**, 10819 (2016).

[26] M. I. Salkola, V. J. Emery, and S. A. Kivelson, Implications of Charge Ordering for Single-Particle Properties of High-T_c Superconductors, Phys. Rev. Lett. **77**, 155 (1996).

[27] A. Lanzara, P. V. Bogdanov, X. J. Zhou, S. A. Kellar, D. L. Feng, E. D. Lu, T. Yoshida, H. Eisaki, A. Fujimori, K. Kishio *et al.*, Evidence for ubiquitous strong electron-phonon coupling in high-temperature superconductors, Nature (London) **412**, 510 (2001).

[28] J. Zaanen, G. A. Sawatzky, and J. W. Allen, Band Gaps and Electronic Structure of Transition-Metal Compounds, Phys. Rev. Lett. **55**, 418 (1985).

[29] C. T. Chen, L. H. Tjeng, J. Kwo, H. L. Kao, P. Rudolf, F. Sette, and R. M. Fleming, Out-of-Plane Orbital Characters of Intrinsic and Doped Holes in $La_{2-x}Sr_xCuO_4$, Phys. Rev. Lett. **68**, 2543 (1992).

[30] N. B. Brookes, G. Ghiringhelli, O. Tjernberg, L. H. Tjeng, T. Mizokawa, T. W. Li, and A. A. Menovsky, Detection of Zhang-Rice Singlets Using Spin-Polarized Photoemission, Phys. Rev. Lett. **87**, 237003 (2001).

[31] N. B. Brookes, G. Ghiringhelli, A.-M. Charvet, A. Fujimori, T. Kakeshita, H. Eisaki, S. Uchida, and T. Mizokawa, Stability of the Zhang-Rice Singlet with Doping in Lanthanum Strontium Copper Oxide Across the Superconducting Dome and Above, Phys. Rev. Lett. **115**, 027002 (2015).

[32] D. I. Khomskii, *Basic Aspects of the Quantum Theory of Solids: Order and Elementary Excitations* (Cambridge University Press, Cambridge, 2010), Sec. 12.10.

[33] *The Physics of Correlated Insulators, Metals, and Superconductors Modeling and Simulation* edited by E. Pavarini, E. Koch, R. Scalettar, and R. Martin (Forschungszentrum Julich, Julich, 2017).

[34] M. Schluter, M. S. Hybertsen, and N. E. Christensen, Calculation of the many body interaction parameters in the high T_c compound La_2CuO_4, Physica C **153-155**, 1217 (1988); M. S. Hybertsen, M. Schluter, and N. E. Christensen, Calculation of Coulomb-interaction parameters for La_2CuO_4 using a constrained-density-functional approach, Phys. Rev. B **39**, 9028 (1989).

[35] H. Eskes, G. A. Sawatzky, and L. F. Feiner, Effective transfer for singlets formed by hole doping in the high-T_c superconductors, Physica C **160**, 424 (1989).

[36] A. K. McMahan, J. F. Annett, and R. M. Martin, Cuprate parameters from numerical Wannier functions, Phys. Rev. B **42**, 6268 (1990).

[37] P. Werner, R. Sakuma, F. Nilsson, and F. Aryasetiawan, Dynamical screening in La_2CuO_4, Phys. Rev. B **91**, 125142 (2015).

[38] M. Hirayama, Y. Yamaji, T. Misawa, and M. Imada, *Ab initio* effective Hamiltonians for cuprate superconductors, Phys. Rev. B **98**, 134501 (2018).

[39] A. Fujimori, E. Takayama-Muromachi, Y. Uchida, and B. Okai, Spectroscopic evidence for strongly correlated electronic states in La-Sr-Cu and Y-Ba-Cu oxides, Phys. Rev. B **35**, 8814(R) (1987).

[40] Z.-X. Shen, J. W. Allen, J. J. Yeh, J.-S. Kang, W. Ellis, W. Spicer, I. Lindau, M. B. Maple, Y. D. Dalichaouch, M. S.

Torikachvili *et al.*, Anderson Hamiltonian description of the experimental electronic structure and magnetic interactions of copper oxide superconductors, Phys. Rev. B **36**, 8414 (1987).

[41] F. Mila, Parameters of a Hubbard Hamiltonian to describe superconducting Cu oxides, Phys. Rev. B **38**, 11358 (1988).

[42] H. Eskes, L. H. Tjeng, and G. A. Sawatzky, Cluster-model calculation of the electronic structure of CuO: A model material for the high-T_c superconductors, Phys. Rev. B **41**, 288 (1990).

[43] M. E. Simon, M. Balina, and A. A. Aligia, Effective one-band hamiltonian for cuprate superconductor metal-insulator transition, Physica C **206**, 297 (1993).

[44] M. E. Simon and A. A. Aligia, Brinkman-Rice transition in layered perovskites, Phys. Rev. B **48**, 7471 (1993).

[45] M. Guerrero, J. E. Gubernatis, and S. Zhang, Quantum Monte Carlo study of hole binding and pairing correlations in the three-band Hubbard model, Phys. Rev. B **57**, 11980 (1998).

[46] D. Senechal, D. Perez, and M. Pioro-Ladriere, Spectral Weight of the Hubbard Model through Cluster Perturbation Theory, Phys. Rev. Lett. **84**, 522 (2000).

[47] A. Go and A. J. Millis, Spatial Correlations and the Insulating Phase of the High-T_c Cuprates: Insights from a Configuration-Interaction-Based Solver for Dynamical Mean Field Theory, Phys. Rev. Lett. **114**, 016402 (2015).

[48] E. W. Huang, C. B. Mendl, S. Liu, S. Johnston, H.-C. Jiang, B. Moritz, and T. P. Devereaux, Numerical evidence of fluctuating stripes in the normal state of high-T_c cuprate superconductors, Science **358**, 1161 (2017).

[49] E. Vitali, H. Shi, A. Chiciak, and S. Zhang, Metal-insulator transition in the ground state of the three-band Hubbard model at half filling, Phys. Rev. B **99**, 165116 (2019).

[50] M. Cini, Density of states of two interacting holes in a solid, Solid State Commun. **20**, 605 (1976); Two hole resonances in the XVV Auger spectra of solids, **24**, 681 (1977); Comment on quasiatomic Auger spectra in narrow-band metals, Phys. Rev. B **17**, 2788 (1978).

[51] G. A. Sawatzky, Quasiatomic Auger Spectra in Narrow-Band Metals, Phys. Rev. Lett. **39**, 504 (1977).

[52] A. Balzarotti, M. De Crescenzi, N. Motta, F. Patella, and A. Sgarlata, Valence charge fluctuations in $YBa_2Cu_3O_{7-\delta}$ from core-level spectroscopies, Phys. Rev. B **38**, 6461 (1988).

[53] D. van der Marel, J. van Elp, G. A. Sawatzky, and D. Heitmann, X-ray photoemission, bremsstrahlung isochromat, Auger-electron, and optical spectroscopy studies of Y-Ba-Cu-O thin films, Phys. Rev. B **37**, 5136 (1988).

[54] L. H. Tjeng, C. T. Chen, and S.-W. Cheong, Comparative soft-x-ray resonant-photoemission study on $Bi_2Sr_2CaCu_2O_8$, CuO, and Cu_2O, Phys. Rev. B **45**, 8205 (1992).

[55] R. Bar-Deroma, J. Felsteiner, R. Brener, J. Ashkenazi, and D. van der Marel, Auger spectra and band structure of $La_{1.85}Sr_{0.15}CuO_4$ and $La_{1.85}Ba_{0.15}CuO_4$, Phys. Rev. B **45**, 2361 (1992).

[56] N. Nücker, E. Pellegrin, P. Schweiss, J. Fink, S. L. Molodtsov, C. T. Simmons, G. Kaindl, W. Frentrup, A. Erb, and G. Muller-Vogt, Site-specific and doping-dependent electronic structure of $YBa_2Cu_3O_x$ probed by O 1*s* and Cu 2*p* x-ray-absorption spectroscopy, Phys. Rev. B **51**, 8529 (1995).

[57] A. M. Oles and W. Grzelka, Electronic structure and correlations of CuO_3 chains in $YBa_2Cu_3O_7$, Phys. Rev. B **44**, 9531 (1991).

[58] M. A. van Veenendaal, G. A. Sawatzky, and W. A. Groen, Electronic structure of $Bi_2Sr_2Ca_{1-x}Y_xCuO_{8+\delta}$: Cu 2*p* x-ray-photoelectron spectra and occupied and unoccupied low-energy states, Phys. Rev. B **49**, 1407 (1994).

[59] A. C. Walters, T. G. Perring, J.-S. Caux, A. T. Savici, G. D. Gu, C.-C. Lee, W. Ku, and I. A. Zaliznyak, Effect of covalent bonding on magnetism and the missing neutron intensity in copper oxide compounds, Nat. Phys. **5**, 867 (2009).

[60] P. Bourges, H. Casalta, A. S. Ivanov, and D. Petitgrand, Superexchange Coupling and Spin Susceptibility Spectral Weight in Undoped Monolayer Cuprates, Phys. Rev. Lett. **79**, 4906 (1997).

[61] S. M. Hayden, G. Aeppli, T. G. Perring, H. A. Mook, and F. Dogan, High-frequency spin waves in $YBa_2Cu_3O_{6.15}$, Phys. Rev. B **54**, R6905 (1996).

[62] M. P. M. Dean, A. J. A. James, R. S. Springell, X. Liu, C. Monney, K. J. Zhou, R. M. Konik, J. S. Wen, Z. J. Xu, G. D. Gu *et al.*, High-Energy Magnetic Excitations in the Cuprate Superconductor $Bi_2Sr_2CaCu_2O_{8+\delta}$: Towards a Unified Description of Its Electronic and Magnetic Degrees of Freedom, Phys. Rev. Lett. **110**, 147001 (2013).

[63] Y. Y. Peng, M. Hashimoto, M. Moretti Sala, A. Amorese, N. B. Brookes, G. Dellea, W.-S. Lee, M. Minola, T. Schmitt, Y. Yoshida *et al.*, Magnetic excitations and phonons simultaneously studied by resonant inelastic x-ray scattering in optimally doped $Bi_{1.5}Pb_{0.55}Sr_{1.6}La_{0.4}CuO_{6+\delta}$, Phys. Rev. B **92**, 064517 (2015).

[64] L. Wang, G. He, Z. Yang, M. Garcia-Fernandez, K. Zhou, M. Minola, M. Le Tacon, B. Keimer, A. Nag, Y. Y. Peng *et al.*, Paramagnons and high-temperature superconductivity in a model family of cuprates, Nat. Commun. **13**, 3163 (2022).

[65] Y. Y. Peng, E. W. Huang, R. Fumagalli, M. Minola, Y. Wang, X. Sun, Y. Ding, K. Kummer, X. J. Zhou, N. B. Brookes *et al.*, Dispersion, damping, and intensity of spin excitations in the monolayer (Bi, Pb)$_2$(Sr, La)$_2CuO_{6+\delta}$ cuprate superconductor family, Phys. Rev. B **98**, 144507 (2018).

[66] R. Neudert, S.-L. Drechsler, J. Malek, H. Rosner, M. Kielwein, Z. Hu, M. Knupfer, M. S. Golden, J. Fink, N. Nucker *et al.*, Four-band extended Hubbard Hamiltonian for the one-dimensional cuprate Sr_2CuO_3: Distribution of oxygen holes and its relation to strong intersite Coulomb interaction, Phys. Rev. B **62**, 10752 (2000).

[67] K. Okada and A. Kotani, Intersite Coulomb interactions in quasi-one-dimensional copper oxides, J. Phys. Soc. Jpn. **66**, 341 (1997).

[68] T. Böske, O. Knauff, R. Neudert, M. Kielwein, M. Knupfer, M. S. Golden, J. Fink, H. Eisaki, S. Uchida, K. Okada *et al.*, High-resolution x-ray-photoemission study of single crystalline $Sr_2CuO_2Cl_2$, Phys. Rev. B **56**, 3438 (1997).

[69] M. A. van Veenendaal, H. Eskes, and G. A. Sawatzky, Strong nonlocal contributions to Cu 2*p* photoelectron spectroscopy, Phys. Rev. B **47**, 11462 (1993).

[70] M. A. van Veenendaal and G. A. Sawatzky, Nonlocal Screening Effects in 2*p* X-Ray Photoemission Spectroscopy Core-Level Line Shapes of Transition Metal Compounds, Phys. Rev. Lett. **70**, 2459 (1993).

[71] K. Okada, Electronic structure of $Nd_{2-x}Ce_xCuO_4$ and $La_{2-x}Sr_xCuO_4$ deduced from Cu $2p$ photoemission and photoabsorption, J. Phys. Soc. Jpn. **78**, 034725 (2009).

[72] S. Johnston, F. Vernay, and T. P. Devereaux, Impact of an oxygen dopant in $Bi_2Sr_2CaCu_2O_{8+\delta}$, Europhys. Lett. **86**, 37007 (2009).

[73] R. Coldea, S. M. Hayden, G. Aeppli, T. G. Perring, C. D. Frost, T. E. Mason, S.-W. Cheong, and Z. Fisk, Spin Waves and Electronic Interactions in La_2CuO_4, Phys. Rev. Lett. **86**, 5377 (2001).

[74] P. W. Leung, B. O. Wells, and R. J. Gooding, Comparison of 32-site exact-diagonalization results and ARPES spectral functions for the antiferromagnetic insulator $Sr_2CuO_2Cl_2$, Phys. Rev. B **56**, 6320 (1997).

[75] C. Kim, P. J. White, Z.-X. Shen, T. Tohyama, Y. Shibata, S. Maekawa, B. O. Wells, Y. J. Kim, R. J. Birgeneau, and M. A. Kastner, Systematics of the Photoemission Spectral Function of Cuprates: Insulators and Hole- and Electron-Doped Superconductors, Phys. Rev. Lett. **80**, 4245 (1998).

[76] H. Jacobsen, S. M. Gaw, A. J. Princep, E. Hamilton, S. Toth, R. A. Ewings, M. Enderle, E. M. Hetroy Wheeler, D. Prabhakaran, and A. T. Boothroyd, Spin dynamics and exchange interactions in CuO measured by neutron scattering, Phys. Rev. B **97**, 144401 (2018).

[77] E. Zurek, O. Jepsen, and O. K. Andersen, Muffin-tin orbital Wannier-like functions for insulators and metals, ChemPhysChem **6**, 1934 (2005).

[78] J. Zaanen and G. A. Sawatzky, The electronic structure and superexchange interactions in transition-metal compounds, Can. J. Phys. **65**, 1262 (1987).

[79] M. Jiang, M. Berciu, and G. A. Sawatzky, Critical Nature of the Ni Spin State in Doped $NdNiO_2$, Phys. Rev. Lett. **124**, 207004 (2020).

[80] Y. F. Kung, C.-C. Chen, Y. Wang, E. W. Huang, E. A. Nowadnick, B. Moritz, R. T. Scalettar, S. Johnston, and T. P. Devereaux, Characterizing the three-orbital Hubbard model with determinant quantum Monte Carlo, Phys. Rev. B **93**, 155166 (2016).

[81] O. J. Lipscombe, S. M. Hayden, B. Vignolle, D. F. McMorrow, and T. G. Perring, Persistence of High-Frequency Spin Fluctuations in Overdoped Superconducting $La_{2-x}Sr_xCuO_4$ ($x = 0.22$), Phys. Rev. Lett. **99**, 067002 (2007).

[82] L. Braicovich, J. van den Brink, V. Bisogni, M. Moretti Sala, L. J. P. Ament, N. B. Brookes, G. M. De Luca, M. Salluzzo, T. Schmitt, V. N. Strocov *et al.*, Magnetic Excitations and Phase Separation in the Underdoped $La_{2-x}Sr_xCuO_4$ Superconductor Measured by Resonant Inelastic X-Ray Scattering, Phys. Rev. Lett. **104**, 077002 (2010).

[83] M. P. M. Dean, R. S. Springell, C. Monney, K. J. Zhou, J. Pereiro, I. Bozovic, B. Dalla Piazza, H. M. Ronnow, E. Morenzoni, J. van den Brink *et al.*, Spin excitations in a single La_2CuO_4 layer, Nat. Mater. **11**, 850 (2012).

[84] G. Levy, M. Yaari, T. Z. Regier, and A. Keren, Experimental determination of superexchange energy from two-hole spectra, arXiv:2107.09181.